ChemComm

Structure-based redesign of Fe(II)/2-oxoglutarate-dependent oxygenase AndA to catalyze spiro-ring formation

Journal:	*ChemComm*
Manuscript ID	CC-COM-02-2022-000736.R1
Article Type:	Communication

COMMUNICATION

Structure-based redesign of Fe(II)/2-oxoglutarate-dependent oxygenase AndA to catalyze spiro-ring formation†

Received 00th January 20xx,
Accepted 00th January 20xx

DOI: 10.1039/x0xx00000x

Takahiro Mori,[a,b,c,‡,*] Yu Nakashima,[a,‡] Heping Chen,[a,‡] Shotaro Hoshino, [a] Takaaki Mitsuhashi,[a] and Ikuro Abe[a,b,*]

Structure- and mechanism-based redesign of the Fe(II)/2-oxoglutarate-dependent oxygenase AndA was performed. The function of AndA was expanded to catalyze a spiro-ring formation reaction from an isomerization reaction. The redesigned AndA variants produced two unnatural novel spiro-ring containing compounds through two and three consecutive oxidation reactions.

Spiro compounds are molecules containing two rings connected by one shared atom. These compounds are present in many natural products, such as the antifungal drug griseofulvin, antimitotic agent spirotryprostatins, bacterial genotoxin colibactin, and cytotoxic spiroindole paraherquamides and notoamides (Fig. S1A).[1] The complexity, chirality, and rigidity of spirocyclic scaffolds have attracted keen attention from synthetic chemists and medicinal chemists for drug discovery. Although some methods for the synthesis of spiro rings have been reported, the regio- and stereo-controlled spiro ring synthesis is still an important challenge.[2] Notably, enzymatic formations of spiro-ring structures have also been identified in secondary metabolite biosyntheses[3]. Several different groups of enzymes, including flavin-dependent monooxygenases[4], Diels–Alderases[5], cytochrome P450s[6], and Fe(II)/2-oxoglutarate dependent oxygenase (2-OGD)[7], catalyze stereo- and regio-selective spiro-ring formation reactions. Furthermore, the chemo-enzymatic syntheses of spiro-rings have been demonstrated by using norcoclaurine synthase[8] and an engineered P450 enzyme[9] *via* Pictet–Spengler and carbene transfer reactions, respectively.

Spiro-ring formation by 2-OGD is observed in the biosynthesis of austinol from *Aspergillus nidulans*. The multifunctional 2-OGD AusE constructs the characteristic spiro-ring through two sequential reactions.[7] The enzyme catalyzes the Δ1,2 desaturation of preaustinoid A1 to produce preaustinoid A2, which is accepted by AusE again to generate the spirolactone-containing preaustinoid A3 (Fig. S2A). Moreover, AusE also accepts preaustinoid A, a biosynthetic precursor of preaustinoid A1, and generates austinoid C with a spiro-cyclopentenone structure via preaustinoid C, with a conjugated Δ1,2 double bond (Fig. S2B and Fig. S3). The structure-function analyses of AusE indicated that the formation of the C-5 radical and conjugated double bond at C1-C2 are important for the formation of the key cyclopropylcarbinyl intermediate (intermediate B and E in Fig. S3A and B) in these spiro-ring formation reactions (Fig. S3A and B). We previously reported the structure-guided engineering of AusE and the homologous enzyme PrhA (78% amino acid identity to AusE) from *Penicillium brasilianum*, which also accepts preaustinoid A1 and catalyzes the desaturation of Δ5,6 and the B-ring expansion reaction to produce berkeleydione, in the biosynthesis of paraherquonin[7] (Fig. S2A). The PrhA-V150L/A232S variants interconverted the catalytic functions to catalyze AusE-type and PrhA-type reactions, respectively.

Although we have successfully engineered the enzymatic functions of the highly similar AusE and PrhA, studies focusing on the functional redesign of 2-OGD are still relatively scarce compared to the number of structure-function studies.[6,7] Therefore, to further demonstrate the enzymatic redesign of 2-OGD, this study focused on AndA of *A. variecolor*, which shows moderate similarity (38% amino acid identity) to AusE, which is significantly lower than the similarity between PrhA and AusE. Furthermore, AndA is well characterized structurally and mechanistically, and it was desirable to engineer the catalytic function of AndA. Thus, we believe that rational modification of the function of AndA to catalyze AusE-like spiro-ring formation could provide clues to expand the versatility and applications of various 2-OGD catalysts in the future.

[a] *Graduate School of Pharmaceutical Sciences, The University of Tokyo, Tokyo, 113-0033, Japan.*
E-mail: tmori@mol.f.u-tokyo.ac.jp, abei@mol.f.u-tokyo.ac.jp
[b] *Collaborative Research Institute for Innovative Microbiology, The University of Tokyo, Yayoi 1-1-1, Bunkyo-ku, Tokyo 113-8657, Japan.*
[c] *PRESTO, Japan Science and Technology Agency (JST), Kawaguchi, Saitama 332-0012, Japan.*
†Electronic Supplementary Information (ESI) available: Experimental methods, crystal statistic table, plasmids, primers, and supplementary figures. See DOI: 10.1039/x0xx00000x
‡ These authors contributed equally to this work.

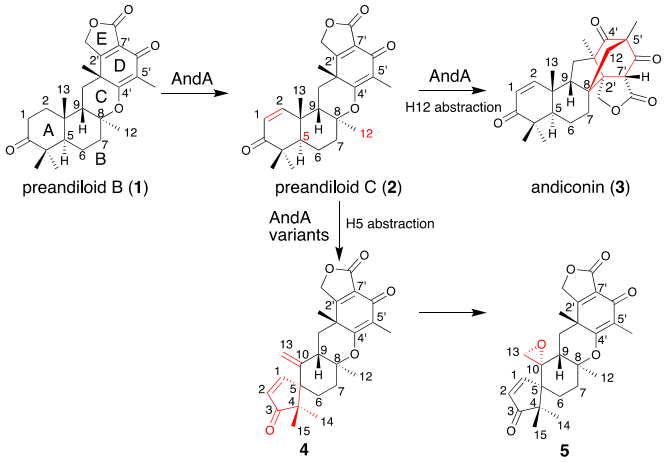

Fig. 1. Enzyme reaction of wild type AndA.

AndA has been identified in the biosynthesis of anditomins and catalyzes the desaturation and isomerization reactions of preandiloid B (**1**) to produce andiconin (**3**) via preandiloid C (**2**) (Fig. 1).[10] The first step of the AndA reaction is the formation of a conjugated Δ1,2 double bond in **2** from **1**, similar to that of AusE. In the following isomerization reaction, the structural analyses and computational calculations suggested that the reaction is initiated by hydrogen atom abstraction from C-12 (intermediate G). The subsequent 1) C-O bond cleavage at C-8 (intermediate H), 2) C-C bond formation between the C-12 and C-5' (intermediate I), and 3) C-C bond formation between C-8 and C-2' generate the bicyclo[2.2.2]-octane ring of **3** (Fig. S3B).

The re-examination of the crystal structure of AndA in complex with **2** revealed that the hydrogen atom at C-5 also faces toward the iron-center, while the methyl group of C-12 is in the closest position to the iron atom (Fig. S4). Furthermore, the A-ring of **2** forms a pseudo-boat conformation due to the conjugated Δ1,2 double bond, resulting in the closer distance between C-1 and C-5. Therefore, we hypothesized that the function of AndA can be altered from the isomerization reaction to the spiro-ring formation reaction by changing the position of hydrogen abstraction from C-12 to C-5. To test this hypothesis, we performed a semirational protein redesign by using structure-guided and site-specific saturation mutagenesis. The structure of AndA with **2** indicated that Asn121 forms a hydrogen bond interaction with the C3-ketone group of **2**, and Met119, Ala228, and Ala230 protrude toward the substrate and determine the shape of the active site (Fig. S4). Therefore, we targeted these residues for random mutagenesis to change the binding mode of **1** in the active site.

The pairs of Met119/Asn121 and Ala228/Ala230 were randomly substituted, and the mutant libraries were expressed in *Escherichia coli*. The enzyme reactions were conducted using crude cell-lysates arrayed in 96-well plates and the enzyme reaction products of individual variants were evaluated by LC-MS. The screening of enzyme reaction products from ~500 colonies revealed that some variants generated the new peak **4**, which is not observed in the wild type AndA reaction. Compound **4** possesses *m/z* 409.2019[M+H]$^+$ (calc. for $C_{25}H_{29}O_5$: 409.2010), indicating the loss of two hydrogen atoms from **2** or

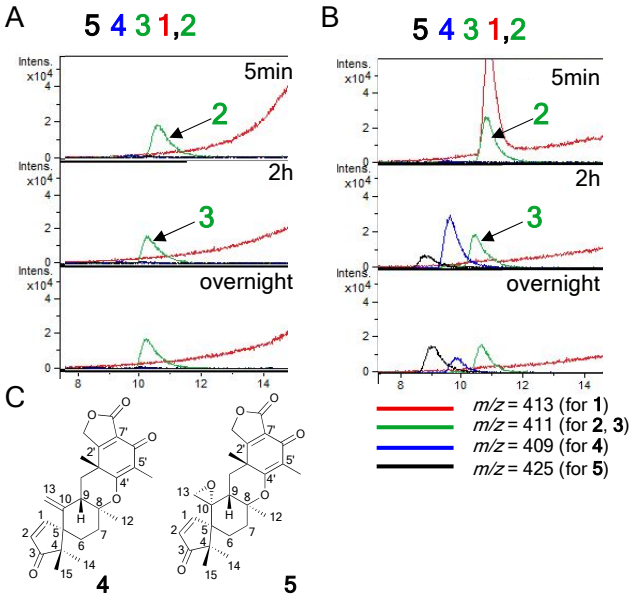

Fig. 2. *In vitro* analysis of AndA wild type and representative variants. EIC of LC-MS chromatograms of (A) AndA wild type and (B) M119A/N121V variant reactions. EIC of LC-MS chromatograms of other variants reactions are shown in Fig. S6. (C) Structures of **4** and **5**.

3 (*m/z* 411) (Fig. S5). Seven **4**-producing variants were selected and subjected to sequence analysis, which indicated that these AndA variants contain the M119C/N121C, M119F/N121V, M119G/N121F, M119G/N121V, A228D/A230G, and A228N/A230S mutations.

Interestingly, a further *in vitro* enzyme reaction with purified enzymes and **1** revealed that five of the seven variants (M119A/N121V, M119C/N121C, M119G/N121F, M119G/N121V, and A228N/A230S) also generated another new product **5**, in addition to **3** and **4** (Figs. 2A and S6, and Table S2). The mass of **5** was *m/z* 425.1969 [M+H]$^+$ (calc. for $C_{25}H_{28}O_6$: 425.1960), which is 16 Da larger than that of **4**, suggesting that **5** is the oxidized product of **4**. Indeed, the time-course reaction of the M119A/N121V variant with **1** revealed that **2** was firstly generated from **1**, and was further converted into **3** and **4**. Finally, **4** was consumed to produce **5**, while **3** was accumulated. (Figs. 2B and S6).

To determine the structures of **4** and **5**, large-scale enzyme reactions using AndA variants were performed. Comparisons of the NMR spectra[‡] between **2** and **4** or **5** indicated that the C-E ring system of **2** was not modified in **4** and **5** (Figs. 2C and S7, Tables S3 and S4). In contrast, the 2D NMR spectra indicated that both **4** and **5** contain a spiro-cyclopentenone scaffold at the A/B-ring moiety (Figs. 2C and S7). Furthermore, the ^{1}H, ^{13}C, and HSQC spectra of **4** showed the presence of an *exo*-olefin structure at C-10 (δC 148.3 ppm) and C-13 (δH 4.81 and 4.86 ppm, and δC 111.8 ppm), which was further supported by the HMBC analysis (Fig. S7). The NOESY correlations of H-9/H1-4 and H-9/H-15 strongly suggested that the absolute configuration of C-5 is *R* (Fig. S8). However, the molecular formula of **5**, the loss of *exo*-olefin protons, and the presence of an additional methylene group (δH 2.41 and 2.76 ppm, and δC 46.5 ppm)

indicated that the C-10-C-13 *exo*-olefin moiety of **4** was converted into the epoxide group in **5** (Fig. S8). To elucidate the stereochemistry of the epoxide ring, we examined the NOESY spectrum of **5** against the low-energy conformers of two possible diastereomers (10*R*/10*S*) obtained by molecular mechanics and quantum mechanics (Fig. S8 and Table S5). As a result, only the low-energy conformers generated from (10*R*)-**5** were consistent with the strong NOESY correlation between H-13 ($^{\delta}$H 2.41 ppm) and H-14 ($^{\delta}$H 1.19 ppm). Furthermore, we also computationally calculated the ^{13}C NMR spectra of possible diastereomers of **5**, and compared them with the experimental spectrum. The DP4+ probability analysis also revealed that the calculated ^{13}C NMR of 10-*R* was consistent with the experimental data (Table S6).[11] Thus, we successfully expanded the function of AndA to catalyze the spiro-ring formation reaction.

Although the reaction from **2** was changed in the AndA variants, the first step of the reaction from **1** to **2** was still conserved. The kinetic analysis of the AndA wild type and AndA M119A/N121V revealed that the k_{cat}/K_M value in AndA M119A/N121V was 2.8 times lower than that of the wild type, while the K_M value in AndA M119A/N121V was 6.9 times higher than that of the wild type (Table S7). The M119A/N121V, M119G/N121V, and M119C/N121C variants, in which Met119 and Asn121 were substituted with smaller and hydrophobic residues, generated the spiro-ring compounds **4** and **5** as the major products. The crystal structure of AndA M119A/N121V revealed that the large-to-small substitutions of Met119 with Ala and Asn121 with Val significantly increased the space at the bottom surface of the active site (Fig. S9)[§]. These observations suggested that an increase in the active site volume around the A-ring of the substrate alters the binding mode, thus moving the H-5 of **2** closer to the catalytic center. However, **4** was not accepted by the M119F/N121V variant. These results suggested that both the loss of the hydrogen bond interaction between Ans121 and the C-3-ketone group and the increase of the space in the active site around Met119 and Asn121 are important to generate **5**. Compound **4** was also produced by the A228N/A230S and A228D/A230G variants, in which the Ala228 residue was replaced with a bulkier and hydrophilic amino acid. The substitution with a hydrophilic residue would form a new hydrogen bond interaction with the C-3 ketone group of **2**, instead of Ans121, which also alters the binding mode of **2**.

In the formation of **4** from **2**, the hydrogen atom at C-5 of **2** is initially abstracted by the ferryl-oxo moiety, instead of H-12, to produce the C-5 radical, as in the AusE reaction (Fig. 3, S2B).[7] Subsequently, the radical rearrangement yields the spiro-ring containing C-10 radical intermediate **C** via a cyclopropylcarbinyl radical intermediate **B**. After the spiro-ring formation at the A/B-ring, the enzyme reaction is terminated by the abstraction of H-13 by the ferric-hydroxy species to form the *exo*-olefin between C-10 and C-13 of **4**, while the H-9 is abstracted in the case of austinoid C formation by AusE. Notably, the stereochemistry of the C-5 atom of **4** (5*S*) is opposite from that of austinoid C (5*R*)[7]. This configuration should be determined by the stereochemistry of the C-13 methyl group in the substrates.

The conformational change of the flexible loop region upon substrate binding has been reported in the AndA enzyme reaction.[10b] Since our crystal structure of AndA M119A/N121V was obtained in the apo-form, the docking simulation of **2** was performed with the model of the closed conformation of AndA M119A/N121V (Fig. 4A). The docking results suggested that the A/B rings of **2** move ~1 Å toward Ala119, while the binding modes of the C/D/E rings are similar to those in the wild type (Fig. S10A). Although the distance between C-5 and the iron center is still 5.4 Å in the docking model, it is possible that the binding conformation of **2** is not completely fixed, due to the loss of the hydrogen bond interaction with Asn121, and C-5 can move closer to the iron center. However, the distance between C-12 and the iron center is 3.6 Å in the docking model, which is

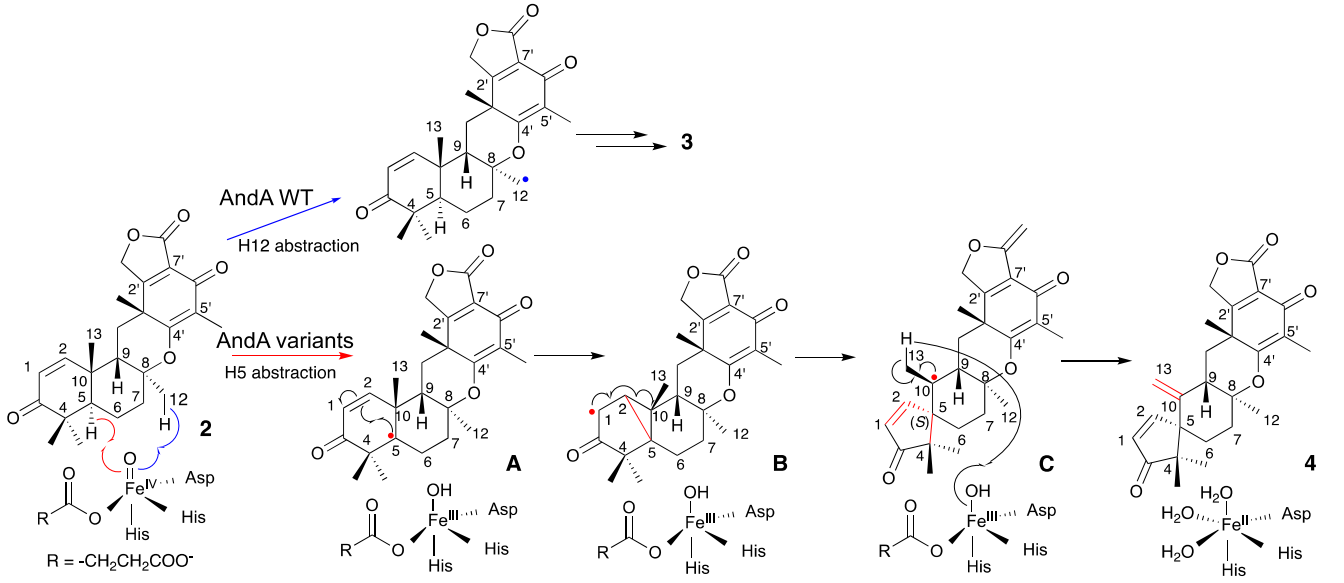

Fig. 3. Proposed reaction mechanisms of spiro-ring formation by AndA variants with **2**. The detailed reaction mechanism of wild type is shown in Fig. S3C.

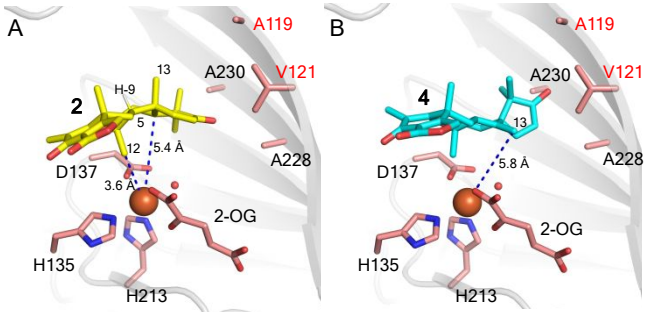

Fig. 4. Docking simulation of AndA M119A/N121V variant. Docking model of AndA M119A/N121V variant (A) with **2** and (B) with **4**. The atom distances are shown as blue dashed lines.

consistent with the production of **3** along with **4** and **5**. The spiro-ring formation reaction is completed by *exo*-olefin formation by H-13 abstraction in the AndA M119A/N121V variant. However, the AndA-Fe/2-OG/**2** complex structure and the docking model of AndA M119A/N121V with **2** indicated that the H-9 atom and C-13 methyl group of **2** protrude in the opposite direction of the iron-center (Fig. 4A). To further clarify the *exo*-olefin formation step, we also performed the docking simulation of **4** with the model of AndA M119A/N121V. The docking structure suggested that the C-10-C-13 bond rotates by ~88 degrees toward the iron center by the formation of the spiro-ring at the A/B-ring, while the position of H-9 does not significantly change (Fig. S10B). As a result, C-13 is in the proximity of the iron at a distance of 5.8 Å, to generate the *exo*-olefin by the hydrogen atom abstraction from C-13 (Fig. 4B). The docking model of AndA M119A/N121V with **4** also suggested that the iron center is located on the re-face of the olefin, which is consistent with the epoxide configuration of (10*R*)-**5**.

The epoxidation reactions catalyzed by 2-OGDs through oxygen atom transfer (OAT) have been well investigated in the enzyme reaction of AsqJ, in the biosynthesis of quinolone alkaloid.[12] The detailed mechanistic analysis of the epoxidation reaction suggested that it most likely proceeds in a stepwise manner via the formation of an Fe-alkoxide species.[12b] In the AndA reaction, the epoxidation of C10-C13 of **4** should be similar to those of other 2-OGDs, in which the initial oxygen addition from the ferryl-oxo to the *exo*-olefin at C-10-C-13 generates an Fe(III)-alkoxide species with a C-10 radical. Then, the formation of the C10-O bond affords the epoxide ring of **5** (Fig. S12).

In conclusion, we have applied structure- and mechanism-guided protein engineering to broaden the reaction scope of AndA. The site of the initial hydrogen atom abstraction was changed by introducing only two mutations, resulting in an AusE-like catalytic capacity to form the spiro-ring structure. The successful expansion of AndA function from the oxidative isomerization reaction to the spiro-ring formation reaction highlights the potential for expanding the catalytic functions of 2-OGD enzymes.

This work was supported in part by a Grant-in-Aid for Scientific Research from the Ministry of Education, Culture, Sports, Science and Technology, Japan (JSPS KAKENHI Grant Number JP16H06443, JP19K15703, JP20H00490, JP20KK0173, and JP20K22700), the New Energy and Industrial Technology Development Organization (NEDO, Grant Number JPNP20011), the PRESTO program from Japan Science and Technology Agency (JPMJPR20DA), AMED (Grant Number JP21ak0101164), Astellas Foundation for Research on Metabolic Disorders, Takeda Science Foundation, and Noda Institute for Scientific Research. We thank Drs. Huiping Zhang and Fumiaki Hayashi for NMR measurements.

Notes and references

‡ NMR data were measured at RIKEN Yokohama NMR Facility.
§ The coordinates and the structure factor amplitudes for the SptF M119A/N121V was deposited under accession code 7WPY.

1 (*a*) L. K. Smith and I. R. Baxendale, *Org. Biomol. Chem.*, 2015, **13**, 9907-9933; (*b*) Y. Zheng, C. M. Tice, and S. B. Singh, *Bioorg. Med. Chem. Lett.*, 2014, **24**, 3673–3682.
2 A. Ding, M. Meazza, H. Guo, J. W. Yang, and R. Rios, *Chem. Soc. Rev.*, 2018, **47**, 5946-5996.
3 M. Tang, Y. Zou, K. Watanabe, C. T. Walsh and Yi Tang, *Chem. Rev.*, 2017, **117**, 5226−5333.
4 (*a*) Y. Tsunematsu, N. Ishikawa, D. Wakana, Y. God2, H. Noguchi, H. Moriya, K. Hotta, and K. Watanabe, *Nat. Chem. Biol.*, 2013, **9**, 818–825; (*b*) A. E. Fraley, K. C. Haatveit, Y. Ye, S. P. Kelly, S. A. Newmister, F. Yu, R. M. Williams, J. L. Smith, K. N. Houk, and D. H. Sherman, *J. Am. Chem. Soc.*, 2020, **142**, 2244-2252; (*c*) T. Matsushita, S. Kishimoto, K. Hara, H. Hashimoto, and K. Watanabe, *Biochemistry*, 2020, **59**, 4787−4792; (*d*) Z. Liu, F. Zhao, B. Zhao, J. Yang, J. Ferrara, B. Sankaran, B. V. V. Prasad, B. B. Kundu, G. N. Phillips Jr., Y. Gao, L. Hu, T. Zhu and X. Gao, *Nat. Commun.*, 2021, **12**, 4158.
5 (*a*) Z. Tian, P. Sun, Y. Yan, Z. Wu, Q. Zheng, S. Zhou, H. Zhang, F. Yu, X. Jia, D. Chen, A. Mándi, T. Kurtán and W. Liu, *Nat. Chem. Biol.*, **11**, 59-65; (*b*) T. Hashimoto, J. Hashimoto, K. Teruya, T. Hirano, K. Shin-Ya, H. Ikeda, H.-W. Liu, M. Nishiyama, T. Kuzuyama, *J. Am. Chem. Soc,*. 2015, **137**, 572−575; (*c*) M.J. Byrne, N. R. Lees, L.-C. Han, M. W. van der Kamp., A. J. Mulholland, J. E. M. Stach, C. L. Willis, and P. R. Race, *J. Am. Chem. Soc.*, 2016, **138**, 6095–6098; (*d*) Q. Li, W. Ding, J. Tu, C. Chi, H. Huang, X. Ji, Z. Yao, M. Ma, and J. Ju, *ACS Omega*, 2020, **5**, 20548−20557.
6 (*a*) X. Zhang and S. Li, *Nat. Prod. Rep.*, 2017, **34**, 1061-1089; (*b*) X. Zhang, J. Guo, F. Chenga and S. Li, *Nat. Prod. Rep.*, 2021, **38**, 1072–1099.
7 (*a*) Y. Matsuda, T. Awakawa, T. Wakimoto, I. Abe, *J. Am. Chem. Soc.*, 2013, **135**, 10962-10965; (*b*) Y. Matsuda and I. Abe, *Nat. Prod. Rep.*, 2016, **33**, 26−53; (*c*) Y. Nakashima, T. Mori, H. Nakamura, T. Awakawa, S. Hoshino, M. Senda, T. Senda, I. Abe, *Nat. Commun.*, 2018, **9**, 104. (*d*) H. Nakamura, Y. Matsuda, I. Abe, *Nat. Prod. Rep.*, 2018, **35**, 633-645.
8 B.R. Lichman, J. Zhao, H.C. Hailes and J. M. Ward, *Nat. Commun.*, 2017, **8**, 14883.
9 K. Chen, S.-Q. Zhang, O. F. Brandenberg, X. Hong and F. H. Arnold, *J. Am. Chem. Soc.*, 2018, **140**, 16402−16407.
10 (*a*) Y. Matsuda, T. Wakimoto, T. Mori, T. Awakawa, I. Abe, I. *J. Am. Chem. Soc.*, 2014, **136**, 15326–15336; (*b*) Y. Nakashima, T. Mitsuhashi, Y. Matsuda, M. Senda, H. Sato, M. Yamazaki, M. Uchiyama, T. Senda, I. Abe, I. *J. Am. Chem. Soc.*, 2018, **140**, 9743-9750.
11 N. Grimblat, M. M. Zanardi, A. M. Sarotti, *J. Org. Chem.*, 2015, **80**, 12526-12534.
12 (*a*) N. Ishikawa, H. Tanaka, F. Koyama, H. Noguchi, C. C. Wang, K. Hotta and K. Watanabe, *Angew. Chem., Int. Ed.*, 2014, **53**, 12880−12884; (*b*) J. Li, H.-J. Liao, Y. Tang, J.-L. Huang, L. Cha, T.-S. Lin, J. L. Lee, I. V. Kurnikov, M. G. Kurnikova, W.-C. Chang, N.-L. Chan and Y. Guo, *J. Am. Chem. Soc.*, 2020, **142**, 6268−6284.